STUDIES OF WATER FLOODED CHALK UNDER HIGH PRESSURE BY USE OF X-RAY COMPUTED TOMOGRAPHY

Eyvind Aker, Karstein Monsen, Fabrice Cuisiat, Harald Westerdahl
Norwegian Geotechnical Institute, P.O. Box 3930 Ullevaal Stadion, N-0806 Oslo, Norway

Tron Golder Kristiansen
BP Norge AS, P.O. Box 197, N-4065 Stavanger, Norway

This paper was prepared for presentation at the International Symposium of the Society of Core Analysts held in Toronto, Canada, 21-25 August 2005

ABSTRACT

Laboratory experiments on chalk cores from outcrop material (Lixhe) have been performed to study fluid displacement and deformation processes in chalk during water flooding. The experiments utilize X-ray computed tomography (CT) imaging to visualize the displacement patterns, measure mechanical deformation and determine the fluid saturation. In addition, acoustic measurements were performed to estimate the wave velocity as a function of fluid saturation and rock deformation. Cylindrical chalk cores were subjected to high isotropic pressure (16 MPa) resulting in instantaneous pore collapse when water entered the core. Both fractured and intact cores were studied and mechanical strain was measured both in the axial and cross-line direction. Strong anisotropic cross-line deformation was observed on both fractured and intact samples during pore collapse. Special techniques had to be developed to take into account matrix compaction and core shortening when analysing the CT images and computing the water saturation. The anisotropic deformation is explained by variable oil saturation and presence of high and low permeable zones in the cores. The X-ray imaging clearly provides additional information that is very valuable when interpreting the flooding experiments.

INTRODUCTION

The behaviour of chalk reservoirs has received considerable attention from several oil companies over the last two to three decades. The chalk has some very special properties compared to other carbonate rock, thus making oil production from chalk reservoir especially challenging. During depletion of a fractured chalk reservoir, the Valhall field outside Norway, a dramatic reduction in permeability by 80% has been observed in some areas of the field. In other areas of the reservoir experiencing same level of depletion, the reduction is much less. During water flooding one expect water to cause a pronounced mechanical weakening of the chalk [1-4], often referred to as “water weakening”. This will influence on the interaction between matrix and fractures in terms of fluid flow, fluid displacement and deformations. One may expect that the weakening of chalk around

fractures will result in additional deformation and loss of fracture permeability. Heterogeneities like “dense zones” will also impact the sweep and deformation of the chalk. Under strong re-pressurisation during water injection the fractures may to some degree reopen close to injectors. In lower porosity and stiffer chalk the thermal cooling may also enhance fracture fluid flow. Understanding all these aspects of production and injection into fractured chalks are of great importance in order to be able to predict the production from the fractured chalk fields and their ultimate recovery.

X-ray computed tomography (CT) imaging has wide applications in modern geosciences. It has become a very useful technique providing non-destructive 3D imaging of the internal structure of rock. The method was introduced in petroleum technology in the 1980s and several scientists have reported core-flooding experiments with the aid of CT imaging. The CT scans have been utilized to map the fluid front during miscible and immiscible displacements and to estimate two- and three-phase fluid saturation [5,6,7]. More recently, water flooding of low permeable chalk by use of CT scanning has been reported in [8,9].

The purpose of this study is to investigate the geomechanical compaction of water flooded chalk and the effect of fractures on the displacement of oil by water. In the experiments presented here the chalk samples were subjected to high isotropic pressure causing an instantaneous collapse of the pore structure when water entered the chalk. The collapse resulted in large compaction and the mechanical deformation was monitored from the CT scans and by separate displacement transducers. One objective was to develop a suitable technique to measure the water saturation by the CT where the effect of compaction and shortening of the core was taken into account. The 3D images from the CT scanner were also used to map the fluid front and internal geological structure and relate them to measured mechanical deformation. We find good correspondence between measured deformation and fluid distribution within the cores.

EXPERIMENTAL SETUP

CT-Scanner

The CT scanner used was a Siemens Somatom Emotion medical scanner. This is a third generation scanner where the energy level can be changed from 90 – 150 kV. The 3D pictures were reconstructed from several cross sectional slices, of 1 mm thickness, that covered the whole length of the core. The reconstruction matrix for each slice was 512 by 512 pixels with a pixel size of 0.1 by 0.1 mm. The thickness of the X-ray beam was 1 mm implying that each volume element (voxel) was 0.1 by 0.1 by 1.0 mm. The CT-scanner measures the attenuation of X-rays beams that have penetrated the rock. The basic measuring quantity in each voxel is the linear attenuation coefficient μ relating the incident X-ray intensity to the remaining intensity after the X-ray has passed through the core. The attenuation coefficients is converted into relative CT numbers as defined by

$$CT = 1000\left(\mu - \mu_{\mathrm{w}}\right)/\mu_{\mathrm{w}} \qquad (1)$$

where μ_w denotes the attenuation coefficient of water. The unit- of equation (1) is Hounsfield (H) and by definition the CT number of water is 0 and air is –1000. For high X-ray energies (>100 kV) the CT numbers are proportional to density.

Sample Core Holder

The chalk core was placed inside a specially designed sample holder permitting simultaneous mapping of fluid distribution from X-ray CT and measurements of elastic wave velocities through the rock [10] (Figure 1). The sample holder is made of a carbon fibre composite because of its low density compared to for example steel when related to its failure strength. Thus the sample holder provides excellent transparency to X-rays and can sustain a maximum internal fluid pressure of 30 MPa. The internal fluid pressure can be divided between pore pressure and effective confining stress depending on the reservoir conditions to be simulated.

The core sample was jacketed with a rubber membrane to isolate the core and the pore fluids from the hydraulic oil providing the confining pressure. A specially designed filter was placed at the inlet and the outlet to distribute the invading and defending fluid evenly along the end surfaces of the core. Piezoceramic transducers and receivers were mounted at the end surfaces of the core to measure the elastic P-wave velocity. The transducers had a central frequency of 500 kHz. The axial deformation of the core was measured by two displacement transducers (LVDT) whose position was opposed to each other in the axial direction of the core.

Rock Samples

The cores were taken from outcrop material of Lixhe chalk (Belgium). The outcrop chalk is representative of the chalk of many reservoirs in the southern North Sea. Two cylindrical cores with diameter of 38 mm and length of 50 mm were drilled out from chalk blocks of outcrop material. In the following the two samples are referred to as Lixhe 1 and Lixhe 2 (Table 1). Lixhe 2 contained a tensile fracture parallel to the axial direction of the core. The fracture was created by imposing a splitting stress at the top of a chalk block. Lixhe 2 was drilled out from the fractured block with the fracture crossing the centre of the core end surfaces. The two halve pieces (separated by the fracture) were carefully kept together in a frame.

Fluids and Pressure

The cores were oven dried at 105°C for at least 24 hours before they were saturated with n-Decane in a vacuum chamber. In addition the cores were flooded with 2 – 3 pore volumes of n-Decan after they were mounted into the core holder to enhance the oil saturation. An isotropic confining stress of 16 MPa was applied to the specimen and oil permeability was measured. The measured permeability of Lixhe 1 (intact) and Lixhe 2 (fractured) is more or less identical (Table 1) and the estimated porosities are also close to each other. Hence, at 16 MPa confining stress the permeability of the fracture is very small. This opposed to Graue et al. [11] who studied oil recovery in chalk with open fractures.

The flooding fluid, brine, was made of distilled water mixed with 100 g NaCl per litre water. The cores were flooded stepwise at a rate of 40 ml/h (0.667 ml/min) with increments of about 0.1 of the total pore volume (PV). Between each flooding step the cores were CT scanned and P-wave velocity was measured. The average flow rate between each injection step was close to that of spontaneous imbibition into oil saturated chalk. The axial deformation was monitored during the whole flooding period. The high confining pressure (16 MPa) resulted in instantaneous pore collapse when brine entered the core. Pore collapse occurs in water saturated chalk at isotropic stress levels much lower than in oil saturated chalk. For Lixhe chalk the pore collapse stress is typically 18 MPa (yield stress) under isotropic loading for oil saturated core and 8 MPa for water saturated core. The density of brine was measured to 1.073 g/ml at 20°C and the density of n-Decane is found in the literature to be 0.73 g/ml (also at 20°C).

Pumps at inlet and outlet controlled the fluid flow. The pump at the outlet provided a constant backpressure of 200 kPa, and the pump at the inlet controlled the flow rate of the injected fluid. The setup allowed for relative large temporal variation in input pressure since the fluid was injected in steps of 0.1 pore volumes at a fixed rate. Between each injection step the inlet pressure was allowed to relax to ensure no flow conditions during CT-scanning and the acoustic measurements.

CT images

The visualization of the fluid-rock structure and the estimation of fluid saturation are based on CT subtraction plots were the base image has been subtracted from the current CT image. The base image is the first CT scan of the oil saturated core before flooding. The result is a map of the change in CT numbers (dCT) that is related to the variation in fluid saturation and rock density only. The subtraction ensures that errors introduced by e.g. beam-hardening effects are minimized. The calculation of fluid saturation from the dCT plots assumes a linear relationship between CT numbers and the density of the fluid-rock system.

RESULTS

Both cores (Lixhe 1 and Lixhe 2) experienced large axial and radial compaction during flooding due to water weakening and subsequent collapse of the pore structure. In order to infer the oil and water saturation from CT scans, we must therefore take into account changes in matrix deformation and density. The increase in CT numbers as brine enters the core is a combination of denser pore fluid replacing n-Decane and higher matrix density due to pore collapse. The following analysis proposes a method for separating these two effects using available data from the CT images and axial deformation measurements. The analysis results in accurate brine saturation profiles where the increase in matrix density is taken into account.

Sample compaction

The axial deformation was measured directly from the LVDTs during flooding. Figure 2 shows the axial strain as a function of elapsed time for Lixhe 1 and 2. The total strain in

the axial direction is about 60 mS and 90 mS for Lixhe 1 and 2, respectively. The notches on the strain records correspond to the start of each injection step. The acoustics and CT images were acquired just before each injection step. The rate of compaction was low enough to assume steady state during data acquisition. The deformation in the cross-line (radial) direction was measured directly from the CT images. This was possible because the cross-line strain was sufficiently large to be accurately measured by the CT scanner. The resolution of the CT scanner in the cross-line direction is approximately 0.1 mm and the maximum compaction in the cross sectional plane was about 1 mm.

Figure 3 shows the cross-line strain of Lixhe 1 (top plot) and Lixhe 2 (bottom plot) before and after flooding. The curves represent the average of the cross-line strain for the central half part of the core. Only middle sections are considered, because pressure transducers and filters at the core end faces prevented cross-line deformation there. Initially, the cross section of the cores was shaped like a circle. During flooding anisotropic strain evolved due to non-uniform pore collapse inside the core. We will discuss this evidence later in the article. The total strain in axial and cross-line direction corresponds to earlier reported deformation measurements of chalk experiencing water weakening [3]

The measured axial and cross-line strains serve as input data to compute the core dry bulk density $\tilde{\rho}_B$ as a function of position along the core for different injection steps. Ahead of the water front $\tilde{\rho}_B$ is assumed to be equal to the initial dry bulk density (found from weighing the core dry). The assumption is supported by the observed piston type displacement of oil by water (e.g. Figure 7). Figure 4 is plotting $\tilde{\rho}_B$ for Lixhe 2 at specific injection steps and similar behaviour is found for Lixhe 1. After 0.3 PV the water front has reached about halfway into Lixhe 2 where the computed bulk density increases sharply from the initial value (1.52 g/cm^3) to about 1.67 g/cm^3 behind the front (Figure 4; solid line). Breakthrough of brine at the outlet was observed after 0.5 PV (Figure 4; dashed line). The dashed-dotted line in Figure 4 corresponds to the estimated bulk density after injection of 1.0 PV brine and creep. The creep is a result of time dependent mechanical deformation of the core that was kept at constant confining pressure for more that 60 hours after flooding was completed. The reduction in $\tilde{\rho}_B$ towards the end faces is due to core mounting preventing cross-line deformation there.

Notice that because of large axial and cross-line deformations the 3D map of CT numbers in the base image of the fluid-rock system does not fit identically to the 3D map of CT numbers in a later image. Axial and cross-line deformation causes axial and cross-line movement of the core relative to the CT scanner. In addition, the compaction causes a later X-ray beam to cover more structure than a corresponding beam from the base image. It is outside the scope of this paper to describe the techniques that were developed to produce as correct CT subtraction plots as possible. We shortly mention that the measurement of axial deformation, known fixation points on the core relative to the CT scanner and image processing methods made it possible to produce relative dCT plots.

Brine saturation

Like $\tilde{\rho}_B$, the density ρ of the combined fluid-rock system is a time dependent function depending on the spatial coordinates *z*, *r* and θ where *z* is pointing along the axial direction of the core and *r* and θ define the cross sectional plane, i.e. $\rho = \rho(z,r,\theta,t)$. In the following we will assume homogeneous deformation in the cross sectional plane so that $\rho = \rho(z,t)$. Here *t* denotes the time according to the injection steps and for convenience we leave it out in the following expressions. Now, let $\rho_f(z) = S_w(z)\rho_w + (1 - S_w(z))\rho_o$ denote the fluid density of the mixed fluids brine (w) and n-Decane (o) at water saturation $S_w(z)$. Further, let $\Delta\rho(z) = \tilde{\rho}_B(z) - \rho_B$ denote the increase in dry bulk density due to pore collapse. Here ρ_B is the initial dry bulk density for the whole core. Then we can deduce the following expression for ρ

$$\rho(z) = \rho_B + \phi\rho_f(z) + \Delta\rho(z)\left(1 - \frac{\rho_f(z)}{\rho_G}\right) \tag{2}$$

where ρ_G is the grain density and ϕ is the initial porosity. The last term in equation (2) is a result of increased density and reduced porosity when the core experiences pore collapse.

The saturation S_w can be expressed by the relative CT numbers like

$$S_w(z) = a \cdot \left\{\langle \mathrm{dCT}\rangle_{r,\theta}(z) - \mathrm{CT_F}(z)\right\} \tag{3}$$

Here $\langle \mathrm{dCT}\rangle_{r,\theta}$ indicates the average of relative CT numbers in the (r,θ) plane, $\mathrm{CT_F}$ is the increase in CT number due the pore collapse and *a* is a scaling factor relating the measured saturation after flooding to the CT numbers. From equation (2) we have that

$$\mathrm{CT_F}(z) = \mathrm{F} \cdot \Delta\rho(z)\left(1 - \frac{\rho_f(z)}{\rho_G}\right) \tag{4}$$

where F is the proportionality factor between the density of the fluid-rock system and CT numbers. We notice that $\mathrm{CT_F}$ is a function of fluid density and hence also S_w. Therefore to compute the saturation we combine equations (3) and (4) and solve for S_w. The parameters *a* and F are found experimentally for each core and the saturation after flooding is found by weighing. The estimated brine saturation after flooding for Lixhe 1 and 2 was 47.4 % and 71.2 %, respectively.

The computed saturation S_w at four different injection steps is shown in Figure 5 for Lixhe 2. A similar result is obtained for Lixhe 1. The shape of S_w is indicating that the displacement is piston-like which is typical for imbibition of water into a strongly water wet chalk [8]. The accuracy of the estimated saturation is poor at distances less than 0.1 and larger than 0.9 relative to the core length, because of the constraints on the cross-line deformation there.

The estimated porosity fraction, total pore volume and brine saturation after flooding for Lixhe 1 and 2 is given in Table 2. Notice that the residual oil saturation after flooding of Lixhe 1 is about 50% while it is only about 30% in Lixhe 2. Further flooding after water breakthrough did not reduce the residual oil saturation.

P-wave velocity

The P-wave velocity was measured in the axial direction of the core at each injection step. Because of the piston type displacement we only consider the velocity before and after flooding where the fluid saturation is homogeneous in the axial direction. For Lixhe 1 the initial P-wave velocity with oil saturated core was 2210 m/s. After flooding with brine the velocity increased to 2280 m/s. For Lixhe 2 the P-wave velocity increased from 2225 m/s to 2400 m/s after flooding. The higher velocity after flooding in Lixhe 2 compared to Lixhe 1 coincides with the higher final water saturation in Lixhe 2 (71.2% for Lixhe 2 compared to 47.4% for Lixhe 1). The changes in P-wave velocity is a result of the combined effects from variation in fluid saturation, rock strength and core density [12].

DISCUSSION

Complete 3D dCT images of the cores were reconstructed but only 2D longitudinal and cross-sectional cuts are provided here. Figure 6 and Figure 7 show the fluid distribution inferred from the CT subtraction plots after injection of 0.4 PV brine into Lixhe 1 (Figure 6) and 0.3 PV brine into Lixhe 2 (Figure 7). The corresponding water saturation is equal to 37.2% in Lixhe 1 and 40.1% in Lixhe 2. The greyscale indicates the local water saturation where light grey to white means high water saturation and dark grey to black means low or no water saturation. The left plot in Figure 6 and Figure 7 is a horizontal longitudinal cut through the centre axis of the core. The right plots show the cross-sectional cuts whose position is indicated with a white vertical dashed line in the left plots.

The dCT plots in Figure 6 (and the base CT image) show that Lixhe 1 contained geological features of denser matrix and reduced porosity. The features are evident in Figure 6 as black bands that are partially intersecting the core. The measured cross-line strain that is plotted in Figure 3 (top panel) has a maximum at about 65 degrees relative to the horizontal. The dashed line in the right panel in Figure 6 corresponds to 65 degrees and it is clear that the average normal direction of the geological features coincides with the direction of maximum strain. Thus the denser features are stiffening the core resulting in anisotropic deformation during brine invasion and pore collapse.

Lixhe 2 contained a tensile fracture to investigate its effect on fluid flow. In Figure 7 it is evident that the fracture influences the shape of the advancing water front. The fracture plane is oriented vertically and in the horizontal cut (left panel) the fracture is penetrating the middle of the plot from left to right. The displacement of oil in and around the fracture is delayed compared to the surrounding matrix, as is also observed towards the outer surface of the core. The cross-sectional cut (right panel) shows that brine is

invading the region outside the fracture first. The measured cross-line strain for Lixhe 2 (Figure 3 bottom plot) has a maximum deformation normal to the fracture orientation. Thus, the region away from the fracture is experiencing strongest pore collapse. This somewhat surprising observation is most likely a result of higher oil saturation inside the fracture and in nearby pores that are stiffening the pore structure there compared to the brine invaded regions. The effect of the fracture on the residual oil saturation in Lixhe 2 is thought to be minor. The higher residual oil saturation in Lixhe 1 is most likely caused by the presence of geological features of denser and less permeable chalk.

CONCLUSION

We have demonstrated the benefits of using computed tomography (CT) imaging during water flooding experiments of water sensitive high porosity and low permeable chalk. The chalk, initially saturated with oil, was subjected to high isotropic stress causing instantaneous pore collapse as water entered the core. The strong subsequent compaction of the core was measured directly from the CT scans in the cross-line direction and with traditional displacement transducers in the axial direction. The CT images mapping fluid distribution and water front evolution inside the core have provided essential information when evaluating the flooding and deformation processes. A tensile fracture intersecting one of the cores in the longitudinal direction was found to have a minor effect on the final oil recovery but strong impact on the radial core deformation. The CT images of the intact core revealed the presence of geological features (heterogeneities) of low porosity and low permeability sections which induces anisotropy. The anisotropy aligned to measured compaction during pore collapse.

ACKNOWLEDGEMENT

This work has received financial support from BP Norge and the Valhall licence partners (Amerada Hess Norge, Norske Shell and Total Norge) and the Norwegian Geotechnical Institute. The permission to publish the results is greatly acknowledged. The opinions presented in this paper do not necessarily represent the view of the Valhall partnership.

REFERENCES

1. Monjoie, A., C. Schroeder, “Charactéristiques mécaniques de la craie du Crétacé Supérieur”, *J. Craie Université de Lille*, France (1989).
2. Risnes, R., H. Haghighi, R.I. Korsnes, and O. Natvik, “Chalk-fluid interactions with glycol and brines”, *Tectonophys.* (2003) **370**, 213-226.
3. Schroeder, C., V. Maury, G. Halle, “Water/chalk interaction: Part II. Results of tests performed in laboratory on Lixhe chalk to calibrate water/chalk models”, SPE 47587, Eurock ’98, Trondheim, Norway, 1998.
4. Heggheim, T., M.V. Madland, R. Risnes, and T. Austad, “A chemical induced enhanced weakening of chalk by seawater”, *J. Petr. Sci. Eng.* (2005) **46**, 171-184.
5. Vinegar, H.J., S.L. Wellington, “Tomographic imaging of 3-phase flow experiments”, *Review Sci. Instr.*, (1987) **58,** 96-107.
6. Fransham, P.B., J. Jelen, “Displacement of heavy oil visualized by CAT scan”, *J. Can. Pet. Technol.*, (1987) **26**, 42-47.

7. Hove, A.O., J.K. Ringen, P.A. Read, ”Visualization of laboratory corefloods with the aid of computerized tomography of X-rays”, *SPE Res. Eng.* (1987) **2**, 148-154.
8. Akin, S., J.M. Schembre, S.K. Bhat, and A.R. Kovscek, “Spontaneous imbibition characteristics of diatomite”, *J. Petr. Sci. Eng.*, (2000) **25**, 149-165.
9. Mogensen, K., E.H. Stenby, D. Zhou, ”Studies of waterflooding in low-permeable chalk by use of X-ray CT scanning”, *J. Petr. Sci. Eng.*, (2001) **32**, 1-10.
10. Monsen, K., and S.E. Johnstad, “Improved understanding of velocity-saturation relationships using 4D computer-tomography acoustic measurements”, *Geoph. Prospecting*, (2005) **53**, 173-181.
11. Graue, A., T. Bogno, B.A. Baldwin, and E.A. Spinler, “Wettability effects on oil-recovery mechanisms in fractured reservoirs”, *SPE Res. Eval. Eng.*, (2001) **4,** 455-466.
12. Gassmann, F., “Über die Elastizität poröser Medien”, *Vierteljahrsschrift der Naturforschenden Gesellschaft in Zürich*, (1951) **96**, 1-23.

TABLES

Table 1. Properties of core samples before flooding

Sample	Porosity fraction	Permeability [md]	Pore vol. (PV) [ml]	Length [mm]	Diameter [mm]
Lixhe 1 (intact)	0.415	1.65	23.4	49.9	37.9
Lixhe 2 (fractured)	0.440	1.95	24.8	49.9	37.9

Table 2. Properties of core samples after flooding

Sample	Porosity fraction	Pore vol. (PV) [ml]	S_w final
Lixhe 1 (intact)	0.356	18.2	47.4
Lixhe 2 (fractured)	0.362	17.9	71.2

FIGURES

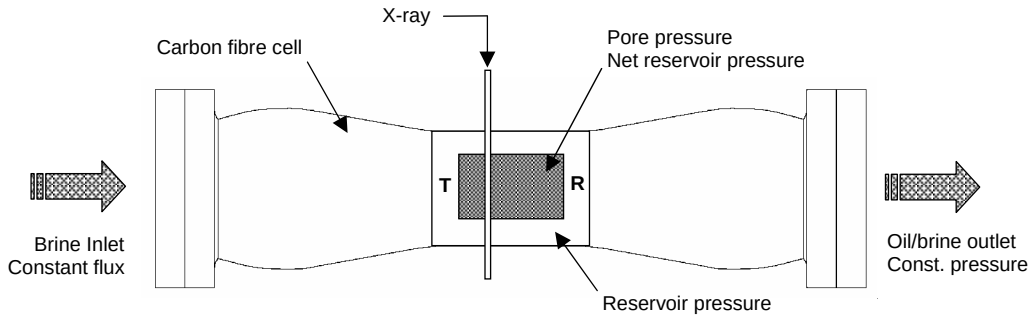

Figure 1. Sample holder. The rock core is located in the centre with acoustic transducer (T) and receiver (R) on the end surfaces. Brine is injected to the left and oil and brine is flowing out to the right. The vertical cut through the core indicates a cross sectional slice

from the X-ray CT-scanner. The core is mapped by several cross sectional slices generating a 3D picture of the rock and fluid.

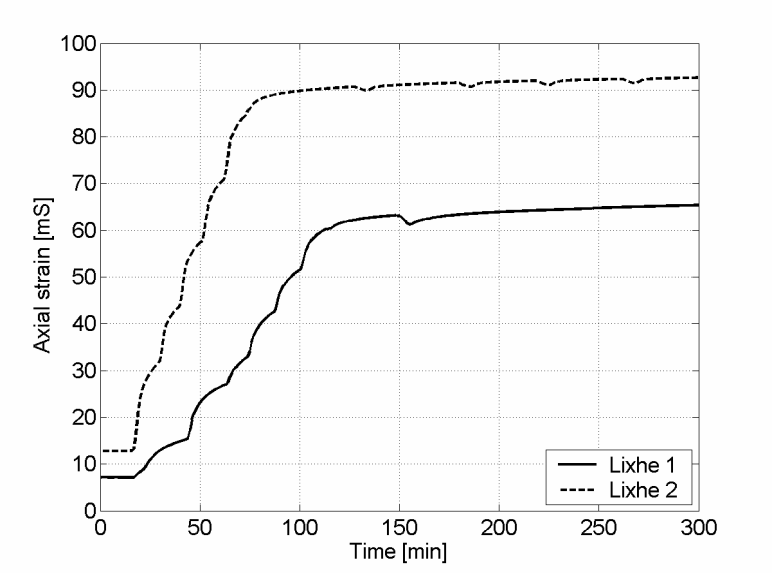

Figure 2. Axial strain versus elapsed time for the brine flooding. The unit is mili-strain, mS

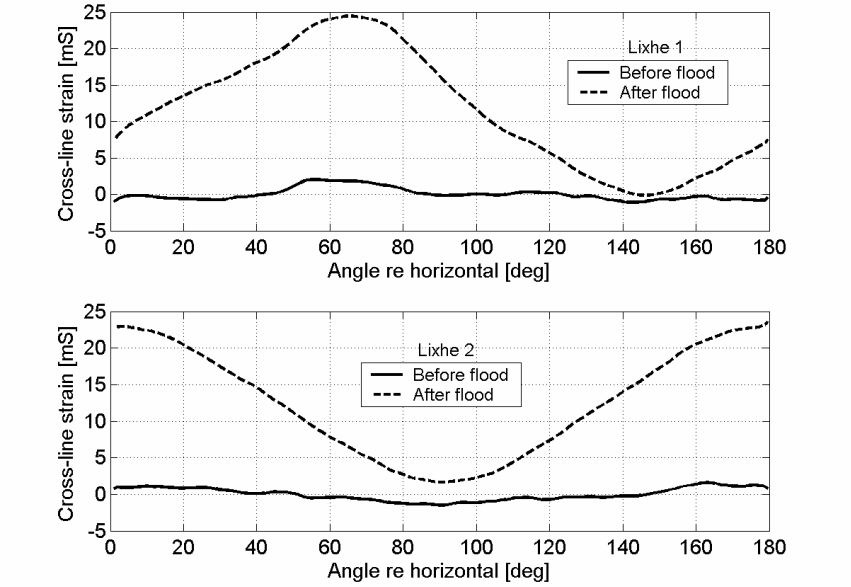

Figure 3. Cross-line strain before (solid line) and after (dashed line) flooding as a function of angle relative to the horizontal. The top panel corresponds to Lixhe 1 while the bottom panel corresponds to Lixhe 2. Initially the cores have a circular cross sectional shape while anisotropic deformations develop during flooding. The unit is mili-strain, mS.

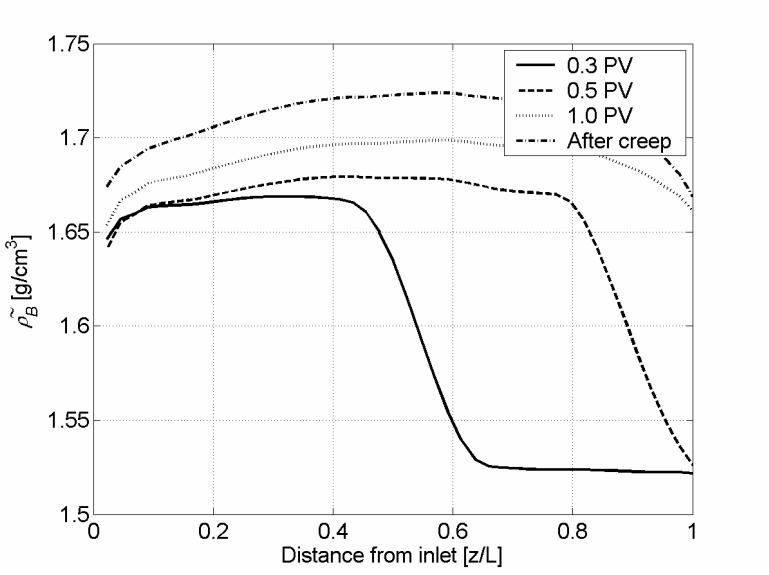

Figure 4. Dry bulk density $\tilde{\rho}_{\mathrm{B}}$ of Lixhe 2 as a function of position *z* along the core at four different times corresponding to injection of 0.3 PV, 0.5 PV and 1.0 PV brine and after a creep phase of 60 hours.

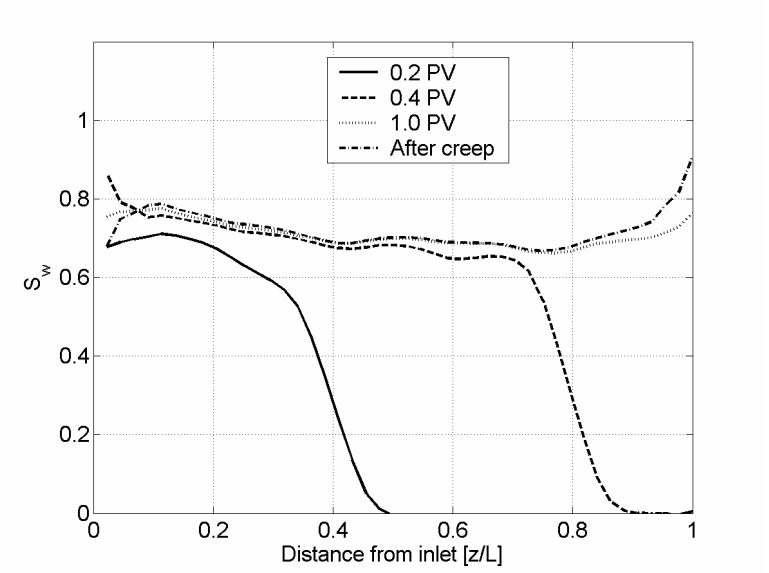

Figure 5. Saturation of brine S_{w} of Lixhe 2 as a function of position *z* along the core at four different times corresponding to injection of 0.2 PV, 0.4 PV and 1.0 PV brine and after a creep phase of 60 hours.

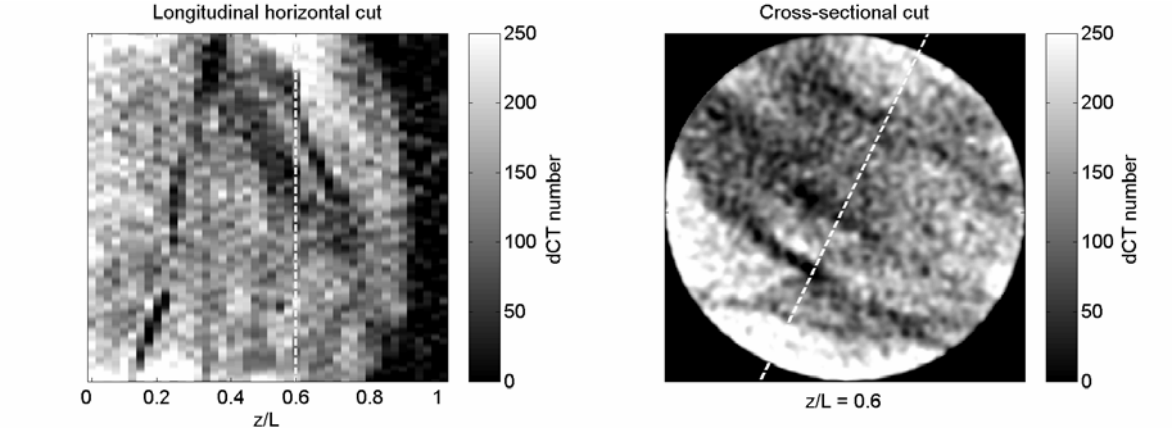

Figure 6. CT subtraction plots (dCT) of Lixhe 1 after injection of 0.4 PV brine. Left panel: A longitudinal horizontal cut through the centre of the core. Right panel: Cross-sectional cut through the core at axial position $z = 0.6L$. The grey scale corresponds to brine saturation where light grey means high saturation and dark grey means low saturation

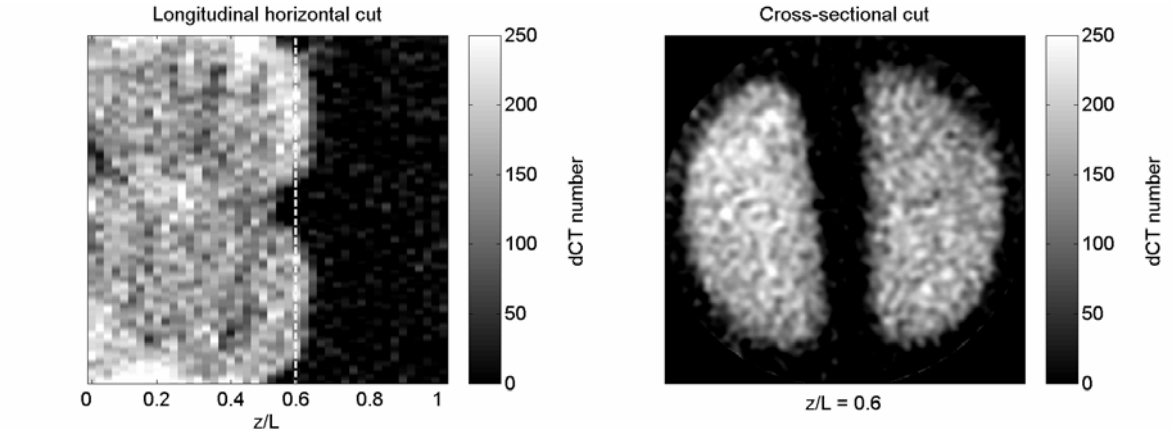

Figure 7. CT subtraction plots (dCT) of Lixhe 2 after injection of 0.3 PV brine. Left panel: A longitudinal horizontal cut through the centre of the core. Right panel: Cross-sectional cut through the core at axial position $z = 0.6L$. The grey scale corresponds to brine saturation where light grey means high saturation and dark grey means low saturation.